Tracking Pore to Pore Exchange Using Relaxation Exchange Spectroscopy

K. E. Washburn and P. T. Callaghan*

MacDiarmid Institute for Advanced Materials and Nanotechnology, School of Chemical and Physical Sciences,
Victoria University of Wellington, New Zealand

(Received 3 May 2006; published 23 October 2006)

We observe the movement of water over time between pores of differing sizes in Castlegate sandstone. To achieve this, we perform an NMR transverse relaxation exchange experiment for several mixing times. The resulting data are converted to 2D T_2 distributions using a 2D inverse Laplace transform (ILT). We show for the first time that quantitative analysis of ILT distributions enables one to extract characteristic times for different pores sizes. This information is potentially useful for permeability determination as well as better understanding of exchange between specific pore subpopulations.

DOI: 10.1103/PhysRevLett.97.175502 PACS numbers: 61.43.Gt, 66.30.Ny, 82.30.Hk, 82.56.Jn

In the physics of soft matter and porous media, a central question concerns the migration of molecules from site to site, under conditions of detailed balance, a process often termed ‘‘exchange.’’ One method of monitoring these processes is by means of nuclear magnetic resonance (NMR), an effective tool being ‘‘2D-exchange NMR’’ [1], in which the NMR spectra, obtained on the same nuclear magnetization but at two successive times, are plotted against each other. Diagonal peaks represent nuclear sites in molecules where properties have remained unchanged, while exchange is indicated by the presence of off-diagonal intensity. Until recently these methods have been restricted to Fourier (frequency domain) spectroscopy, yet many interesting NMR properties are associated with exponential decays, for example, through relaxation and diffusion measurement, for which inverse Laplace transformation (ILT) is the natural domain of analysis. Here we demonstrate for the first time how 2D ILT may be used to quantitatively monitor molecular exchange processes, choosing as a simple example the relaxation-relaxation exchange for liquid molecules imbibed in a porous medium.

In porous media, nuclear spin relaxation in liquid-state molecules is enhanced by collision with pore surfaces, a consequence of a momentary impulse in the dipole-dipole interactions. Consequently, spin-relaxation rates provide a ‘‘marker’’ for pore surface-to-volume ratios and hence pore size distributions [2]. This effect makes NMR of especial use in well-logging tools. In principle, change of spin-relaxation rates as molecules exchange from pore to pore could provide insight regarding interpore transport. The 2D exchange method for tracking molecular migration, which we demonstrate here, is based on relaxation-relaxation comparison. However, it is equally applicable to diffusion-diffusion comparison using pulsed gradient spin echo NMR [3,4]. We do note that relaxation measurements may have particular value in well-logging applications, given that rock permeability may be indirectly deduced from empirical scaling laws based on spin-relaxation time and porosity data [5]. Whether used for soft matter applications (e.g., exchange between liquid crystal domains), in biophysics (exchange of metabolites between the interior and exterior of cells) or in porous media studies (migration between pores), the ability to quantify details of exchange between specific subpopulations could prove of significant value.

In the example presented here, we correlate at two different times, the distribution of molecules in pores, as indicated by their spin-spin (T_2) relaxation properties. The NMR method preserves the magnetization of individual molecules over a variable ‘‘mixing time’’ separating the two intervals when relaxation behavior influences the spin magnetization (we call these intervals during which spin echo rf pulses are applied relaxation time ‘‘encodings’’). Consequently, a switch of T_2 identities over the mixing time indicates molecular exchange, as molecules diffuse from one environment to another. At the heart of the method is the 2D ILT [6], allowing multiexponential signal decays associated with spin relaxation to be converted to 2D relaxation time distributions [7,8]. Off-diagonal peaks tell us where molecules have moved between pores of differing relaxation times. It is the sensitivity of these peaks to mixing time variation which yields pore exchanges times directly.

2D ILT methods have been used in exchange measurement by Callaghan and Furo [9] and Qiao *et al* [10] who observed molecular migration between differing domains in lyotropic liquid crystals and polyelctrolyte capsules, respectively. McDonald and Korb [11] and Lee *et al* [12] have performed a double T_2 encoding at a fixed time separation, which demonstrated the movement of water between differing environments, although no quantitation was attempted.

We here use a range of mixing times to observe the movement of water, extracting exchange rates between subpopulations. The NMR pulse sequence used is shown in Fig. 1. It begins with a 90° excitation rf pulse to place the magnetization in the transverse plane, followed by the first T_2 encoding in the form of a Carr-Purcell-Meiboom-Gill (CPMG) echo train. Note that we keep the echo time fixed (at 25 μs) and vary the number of refocusing 180°

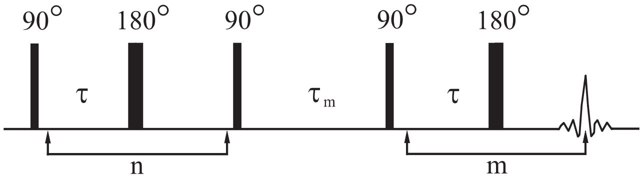

FIG. 1. Two-dimensional pulse sequence for the fast measurement of transverse relaxation exchange. The time interval τ is kept fixed and the numbers (n, m) of 180° rf pulses in the first and second T_2 encoding periods are independently varied. The measurement is performed as a function of the mixing time τ_m.

pulses in the train. The use of closely spaced 180° rf pulses avoids [13] any influence from internal diamagnetic susceptibility differences which can lead to additional dephasing of the transverse magnetization, a problem when performing NMR measurements on a porous medium.

After the first T_2 encoding interval, using 42 logarithmically spaced echo train durations over the range 0.05 to 51.2 ms, a second 90° rf pulse is used to store the magnetization along the z axis for the mixing time, τ_m, where it experiences no further T_2 relaxation, only the longer T_1 relaxation. Mixing times used were 1, 10, 20, 30, 40, 60, 80, 120, and 160 ms, the latter being the upper limit, since at longer times the data become significantly T_1 weighted. At the end of τ_m, a third 90° rf pulse returns the magnetization to the transverse plane where the second T_2 encoding is performed in conjunction with multiecho data acquisition. This enables efficient use of experiment time, a single mixing time experiment taking 12 min, and yielding a signal-to-noise ratio $\gtrsim 100$. rf pulse phase cycling ensures that all signal derives from the first 90° pulse alone. Using single point acquisition the top of each of the 1024 CPMG echoes was sampled, giving a (42×1024) 2D data set. From that set we select second-encode durations corresponding to first-encode times to produce a 42×42 matrix, which is subsequently inverse Laplace transformed to generate a 32×32 T_2-T_2 distribution matrix. In this exchange distribution, molecules that remain in their original environment will appear along the diagonal while those diffusing to a new environment during τ_m will have relaxation time coordinates that are a combination of the two environments (off-diagonal peaks). Note that T_1 values, while longer than T_2, do tend to follow the same size ordering. While detailed balance would suggest cross peak symmetry, the inevitable T_1 relaxation that occurs during the mixing interval of "z storage" means that the cross peaks will not necessarily have equal intensity.

Ideally the T_2 encode times should be less than the exchange times to be measured; otherwise a significant number of molecules can diffuse from one environment to another during the encoding process, causing averaging between T_2 values and smearing of peaks in the T_2 distribution. For the present study, Castlegate sandstone was chosen for its short T_2 relaxation times, in each case considerably less than T_1.

Experiments were performed at 25 C using a Bruker Avance 400 MHz spectrometer with 25 mm proton resonator. Rock cores were saturated in distilled water and excess water carefully removed from the surface before experimentation. The 2D inverse Laplace transforms were performed using Prospa (magritek, Wellington, New Zealand) which incorporates a 2D non-negative least squares algorithm [14]. Regularization involves a curvature cost-benefit function whose amplitude is adjusted to just minimize chi squared. An x-ray computerized tomography (CT) image [15] of the rock is shown in Fig. 2 (right inset), from which a pore size distribution has been derived using the maximal inscribed spheres method [16]. As apparent in Fig. 2, four distinct T_2 contributions can be seen at approximately 0.2 ms (labeled A), 1.6 ms (labeled B), and 8 ms (labeled C), along with a 32.6 ms component labeled D. The discreteness of this distribution is a consequence of ILT "pearling" [14]. A projection from a T_1-T_2 correlation experiment was used to obtain the T_2 spectrum.

Figure 3 shows the 2D T_2 exchange distribution for a 160 ms mixing time. For the 0.2, 1.6, and 8 ms peaks, exchange between T_2 environments is quite evident. Remarkably there is no apparent exchange between the 32.6 ms peak and those associated with shorter T_2 values. The T_2 encoding times are less than or on the order of the exchange times found here. A side effect of limiting the relaxation encoding period is that some of the peak positions appear at spuriously low relaxation times in the 2D T_2 distribution, but their behavior appears otherwise unaffected. To confirm that the cross peaks do indeed arise

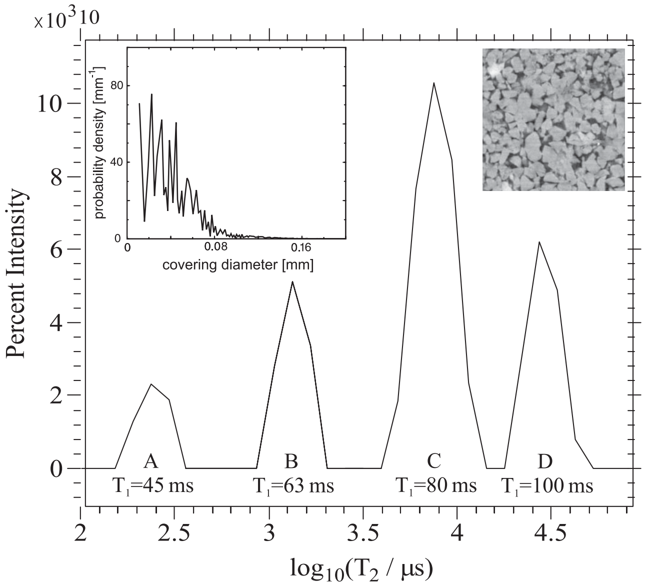

FIG. 2. 1D projection (along T_1) of the $T_1 - T_2$ 2D correlation spectrum. The right inset shows an x-ray CT image of the Castlegate sandstone core, field of view width, 2 mm. The left inset gives the pore size distribution derived from x-ray CT.

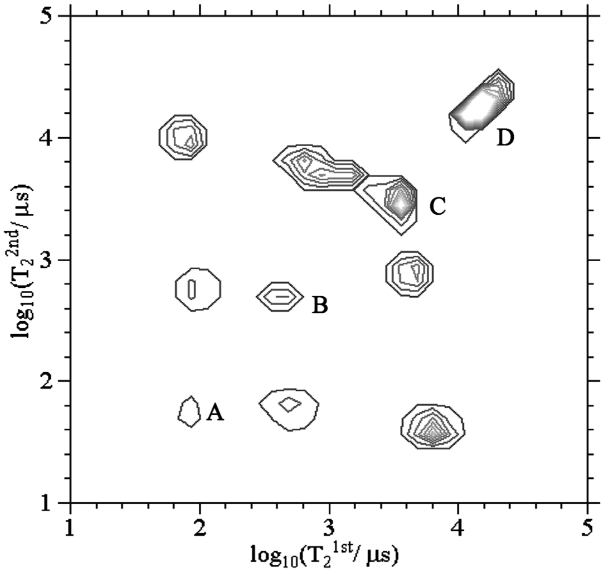

FIG. 3. 2D T_2 exchange distribution for a 160 ms mixing time.

from pore to pore exchange, we turn to quantitative analysis of the data. Simulation of multiexponential time domain data in which exchange occurs between two or three Gaussian distributions of T_2 values has confirmed that the ILT peak intensities closely represent their contribution to the known time domain signal contribution.

Consider sites A and B with equilibrium occupancies, N_A and N_B. Allowing exchange we may write that the numbers of molecules, N_{AB}, starting in A but residing in B after a time delay t will be governed by the rate equation $dN_{AB}/dt = N_{AA}/\tau_{AB} - N_{AB}/\tau_{BA}$, where N_{AA} is the number remaining in A after time t. A similar relation governs transition from B to A simply by exchanging indices. Taken together, these two first order equations imply exponential solutions. Clearly the times τ_{AB} and τ_{BA}, respectively, the rates at which molecules in A migrate to B and vice versa, will be related to the intrinsic molecular self-diffusion coefficient, the tortuosity of the interpore pathway (the pore-pore throat) and the squared interpore distance. $N_{AB}(t)$ ideally corresponds to the A-B off-diagonal peak intensity at mixing time t and has an initial condition $N_{AB}(0) = 0$. Conserving molecules ($N_{AA} + N_{AB} + N_{BB} + N_{BA}$ constant) one may simply show

$$N_{AB}(t) = \frac{N_B \tau_{AB}}{\tau_{AB} + \tau_{BA}}[1 - \exp(-\lambda t)], \tag{1}$$

with $\lambda = \tau_{AB}^{-1} + \tau_{BA}^{-1}$ and $\tau_{\mathrm{ex}}^{AB} = \lambda^{-1}$, while the time-dependent diagonal intensities are given by

$$N_{AA}(t) = \frac{N_A}{\tau_{AB} + \tau_{BA}}[\tau_{AB} - \tau_{BA} \exp(-\lambda t)] \tag{2}$$

and similarly for $N_{BB}(t)$.

Because we are here dealing with three sites, A, B, and C, that mutually exchange (the equations above should be appropriately modified) especially if mixing times are long enough for three site processes to play a significant role. The expressions for $N_{\alpha\alpha}(t)$ and $N_{\alpha\beta}(t)$ (where α is A, B, or C) are more complex than those given here but are easily derived. For simplicity and for pedagogical reasons, we prefer to restrict our approach to a first order analysis and treat the experiment in terms of a set of independent two-site binary exchanges. The fact that the data appear approximately single exponential lends credence to that approach.

Figure 4 shows the integrated off-diagonal peak intensities $N_{\alpha\beta}(t)$ as a function of mixing time, while Fig. 5 shows the diagonal behavior $N_{\alpha\alpha}(t)$. Reproducibility of the data was good. Variations of peak intensity between repeated experiments for the same exchange times were generally a few percent, and this is reflected in the error bars. We note that the intensities $N_{\alpha\alpha}(t)$ of the diagonal peaks, A, B, and C, decreased as decaying exponentials, while for the exchange peaks, $N_{\alpha\beta}(t)$, the intensities grew exponentially, in accordance with Eqs. (1) and (2). Focusing on Fig. 4 and using Eq. (1), we determine the exchange times between the peaks as $\tau_{\mathrm{ex}}^{AB} = 17(2)$ ms, $\tau_{\mathrm{ex}}^{AC} = 21(1)$ ms, and $\tau_{\mathrm{ex}}^{BC} = 43(2)$ ms. These effective exchange times, however, are weighted by T_1 relaxation, as

$$\frac{1}{\tau_{\mathrm{ex}}^{\mathrm{eff}}} = \frac{1}{T_1} + \frac{1}{\tau_{\mathrm{ex}}}. \tag{3}$$

Using the T_1 values from the T_1-T_2 correlation experiment and Eq. (3) we arrive at the actual exchange values $\tau_{\mathrm{ex}}^{AB} = 27(3)$ ms, $\tau_{\mathrm{ex}}^{AC} = 31(3)$ ms, and $\tau_{\mathrm{ex}}^{BC} = 93(11)$ ms. These results are consistent with our simple picture based on pore to pore exchange, given a majority of pores smaller than 50 μm, and the known diffusion coefficient of water.

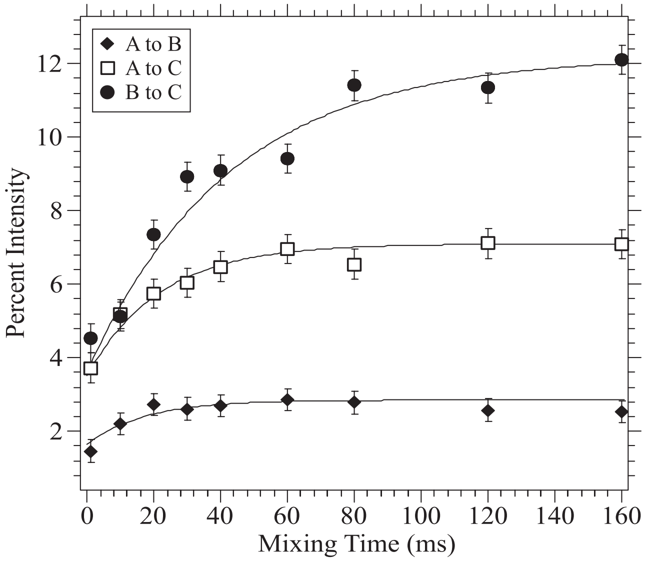

FIG. 4. Off-diagonal intensities, $N_{\alpha\beta}(t)$, as a function of mixing time.

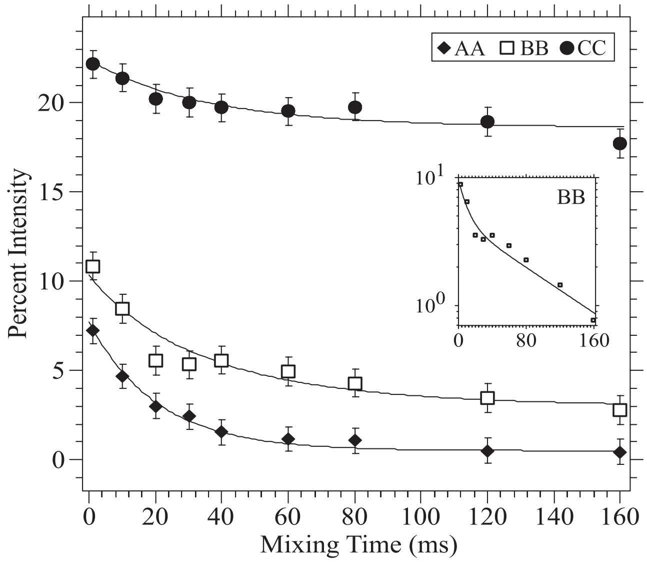

FIG. 5. Intensities, $N_{\alpha\alpha}(t)$, of diagonal peaks A, B, and C. Note that peak D exhibited an intensity constant at around 32%. The semilogarithmic inset shows the biexponential character of $N_{BB}(t)$.

We suggest that the shortest T_2 values (sites A) arise from water molecules in pore throats. It is then reasonable that these $\tau_{\rm ex}^{AB}$ and $\tau_{\rm ex}^{AC}$ exchanges are fastest and of similar rate. We propose that the long exchange time $\tau_{\rm ex}^{BC}$ arises from exchange between true pores of differing sizes. A surprise was the lack of exchange between the longest relaxation peak and the smaller pores. Comparison with results obtained using (otherwise undesirable) longer T_2 encoding times confirm that this is not an exchange process simply missed by the short T_2 encoding times. Indeed, the peak intensity remained nearly constant throughout the range of mixing times. We suggest that in the Castlegate sandstone used here, the relaxation component D arises from water in pores too large for significant exchange on the encoding time scales. This length scale must be $\gtrsim 50$ μm, consistent with the largest pores seen in x-ray CT [16].

Turning to the $N_{\alpha\alpha}(t)$ data of Fig. 5, we might expect, on closer scrutiny, to see biexponential behavior as molecules are lost to either of the two different pore sites. This biexponential character is evident for site B because of its very different exchange times with A and C. While our data do not realistically permit a full biexponential fit, the theory line drawn through the $N_{\alpha\alpha}(t)$ data has time constants preassigned to the values measured for the off-diagonal peaks. The correspondence with the data is excellent.

The data shown here indicate that 2D ILT methods, based on nuclear spin-relaxation times, can provide effective quantitative insight regarding pore-pore exchange in porous media and that, in contrast to 1D methods, exchange between identifiable subpopulations is readily observed. The 2D T_2 relaxation exchange method has the possibility to predict permeability more accurately than the current 1D T_2 methods. The methods described here are time efficient and undemanding of apparatus. They could be readily applied in bore-hole logging applications. While we have chosen to demonstrate the method on a rock core, we would emphasize that the technique is applicable to other porous or compartmented systems such as those found in biology, materials research, and chemical engineering.

The authors are grateful for financial support from the New Zealand Foundation for Research, Science, and Technology. We thank Christoph Arns for helpful discussions and x-ray CT analysis, SINTEF for the Castlegate sample, and Craig Eccles for computational help.

---

*Electronic address: paul.callaghan@vuw.ac.nz

[1] R. R. Ernst, G. Bodenhausen, and A. Wokaun, *Principles of Nuclear Magnetic Resonance in One and Two Dimensions* (Oxford University Press, Oxford, 1987)
[2] R. L. Kleinberg and M. A. Horsfield, J. Magn. Reson. **88**, 9 (1990).
[3] E. O. Stejskal and J. E. Tanner, J. Chem. Phys. **42**, 288 (1965).
[4] P. T. Callaghan, *Principles of Nuclear Magnetic Resonance Microscopy* (Oxford University Press, Oxford, 1991).
[5] K-J. Dunn, G. A. LaTorraca, and D. J. Bergman, Geophysics **64**, 470 (1999).
[6] L. Venkataramanan, Y. Q. Song, and M. D. Huerlimann, IEEE Trans. Signal Process. **50**, 1017 (2002).
[7] Y. Q. Song and L. Venkataramanan, J. Magn. Reson. **154**, 261 (2002).
[8] P. T. Callaghan, S. Godefroy, and B. N. Ryland, Magn. Reson. Imaging **21**, 243 (2003).
[9] P. T. Callaghan and I Furo, J. Chem. Phys. **120**, 4032 (2004).
[10] Y. Qiao, P. Galvosas, T. Adalsteinsson, M. Schoenhoff, and P. T. Callaghan, J. Chem. Phys. **122**, 214912 (2005).
[11] P. J. McDonald and J. P. Korb, Phys. Rev. E **72**, 011409 (2005).
[12] J. H. Lee, C. Labadie, C. S. Springer, and G. S. Harbison, J. Am. Chem. Soc. **115**, 7761 (1993).
[13] B. Sun and K-J. Dunn, Phys. Rev. E **65**, 051309 (2002).
[14] S. Godefroy and P. T. Callaghan, Magn. Reson. Imaging **21**, 381 (2003).
[15] C. H. Arns, A. P. Sheppard, M. Saadatfar, and M. A. Knackstedt, in Proceedings of the 47th Annual Logging Symposium of the Society of Petrophysicists and Well Log Analysts, Veracruz, 2006 (to be published).
[16] C. H. Arns (private communication).